

# Audio Signature-Based Condition Monitoring of Internal Combustion Engine Using FFT and Correlation Approach

Sandeep Kumar Yadav, Kanishka Tyagi, Brijeshkumar Shah, and Prem Kumar Kalra, *Senior Member, IEEE*

**Abstract**—This work proposes a novel prototype-based engine fault classification scheme employing the audio signature of engines. In this scheme, Fourier transform and correlation methods have been used. Notably, automated audio classification has immense significance in the present times, used in both audio-based content retrieval and audio indexing in multimedia industry. Likewise, it is also becoming increasingly important in automobile industries. It has been observed that real world automobile engine audio data are contaminated with substantial noise and out fliers. Hence, it is challenging to categorize different fault types in different engines. Accordingly, the present paper discusses a methodology where a set of algorithms checks the state of an unknown engine as either healthy or faulty. Fault categorizing algorithm is based on its cross- and autocorrelation coefficient values. Appropriately, in this study, the engine amplitude–frequency values of fast Fourier transform are calculated and subdivided into bands to calculate the correlation coefficient matrix. The correlation coefficient matrix for the unknown engine is then calculated and matched with this “prototype” engine matrix to categorize it into a single or multiple fault(s). It is worth mentioning here that although a rank-based maximum close scheme is adopted for finding the unknown engine’s fault, the work can be extended to any other parametric and neural network-based classification scheme. Keeping this background in mind, the present paper discusses the proposed methodology to find a prototype engine, unknown engine classification, implementation on real audio signal for single cylinder engine data, and its results.

**Index Terms**—Condition monitoring, correlation, fault diagnosis, Fourier transform.

## I. INTRODUCTION

THE AUTOMOTIVE industry in the recent past has paid considerable attention to internal combustion (IC) engine condition monitoring since it helps to prevent serious damage by checking the status of the engine. Initially, the condition monitoring of the IC engine depended on the experience of skilled technicians, but the decision making process was highly subjective. Hence, the conventional method proved to be time

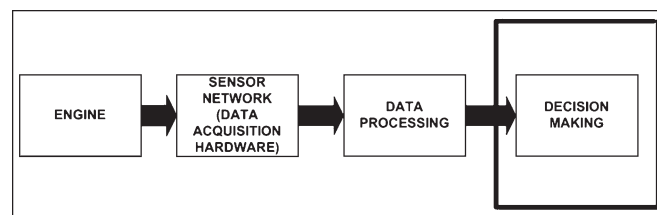


Fig. 1. General Framework for Fault Diagnosis.

consuming and somewhat unreliable. In order to monitor the quality of an IC engine, a robust technique was, therefore, needed to detect its faults.

It is worth mentioning here at this juncture that “health” is a monotonic function over time that eventually crosses a threshold resulting into a fault state. Notably, monotonicity is interrupted by maintenance and accelerated by heavy use. Foregrounding the need for damage prevention, scientific thinkers have presently shown a keen interest in the problem of health and condition monitoring of high value engineering systems. Accordingly, knowledge-based techniques are used to prolong the life of systems by enabling preventive and predictive maintenance which is performed when required. This results in maximum use of components without affecting the availability or the safe operation of the system, and accurate diagnosis of faults.

The other important efficiency enhancing technique is termed as condition-based monitoring (CBM). The three key elements of effective CBM are: 1) **data acquisition**, or the collection and storage of the machine’s health data; 2) **data processing**, or the conditioning and feature extraction/selection of the acquired data; and 3) **decision making**, or recommendation of maintenance actions through diagnosis.

Fig. 1 shows the general framework used in the fault diagnosis. It can be observed here that the sensor network collects the data. Subsequently, data processing and decision making are done by software.

It is reported that 99% of mechanical failures are preceded by noticeable indicators [1]. Over the recent decades, there has been significant advancement in technologies dealing with machine condition monitoring and fault diagnosis. For instance, various data types such as vibration signatures, acoustic signatures, etc., can be acquired and processed through more advanced sensors and robust softwares. Among these, the most widely employed technique for condition monitoring and diagnosis of bearings is vibration monitoring. This is evidenced in

Manuscript received May 24, 2009; revised October 30, 2009; accepted October 31, 2009. Date of publication November 9, 2010; date of current version March 8, 2011. This work was supported by Technology Information, Forecasting and Assessment Council, Department of Science and Technology, Government of India, under project TIFAC/EE/20070174. The Associate Editor coordinating the review process for this paper was Dr. Jesús Ureña.

S. K. Yadav, B. Shah, and P. K. Kalra are with the Department of Electrical Engineering, Indian Institute of Technology Kanpur, Kanpur 208 016, India (e-mail: sandeepy@iitk.ac.in; shahbrij@iitk.ac.in; kalra@iitk.ac.in).

K. Tyagi is with University of Texas at Arlington, Arlington, TX 76019 USA (e-mail: kani@iitk.ac.in).

Color versions of one or more of the figures in this paper are available online at <http://ieeexplore.ieee.org>.

Digital Object Identifier 10.1109/TIM.2010.2082750

the numerous research conducted in this area [2]–[7]. Significantly, acoustic signals are preferred over others since they are airborne. The sensor used in this case is a microphone converting sound waves to electric signal (voltage). As in the case of vibration measurements, a sensor need not be mounted on the surface of an engine. The main disadvantage of acoustic signal is, however, its nonlocalization property. This implies that although it is possible to detect different operating conditions using acoustic signal, it is not possible to localize or detect a specific event which gets complicated due to the increased number of sound sources. The other disadvantage with using vibration signals is that by the time a significant change in vibration is observed, the remaining operational or useful life of an equipment gets significantly reduced. This is where acoustic emission or audio signatures offer a significant advantage. The melange of such new technologies creates a large scope for new forms of information to be analyzed. Accordingly, the research community has at its disposal new concepts to synthesize, analyze, and integrate the information into and create modern reliability and maintenance scheduling scheme.

Importantly, it is observed that there are three main areas in fault diagnosis: 1) **fault detection**—the indication that something is going wrong with the machine; 2) **fault isolation**—determination of the exact location of the fault; and 3) **fault identification**—determination of the size and type or nature of the fault. Some important findings concerning this are given below.

Bunks *et al.* [8] have used the hidden Markov model in the application of CBM. They compared CBM with speech processing and used the Westland helicopter gearbox data set to demonstrate examples of torque level, defect level, and defect-type classifications. They concluded that a distinctly robust classification is shown when the signal-to-noise ratio is low.

Similarly, Yen *et al.* [9] have explored the feasibility of applying the wavelet packet transform to the classification of vibration signals. A unique feature selection process that uses signal class differences in the wavelet packet node energy was implemented. This results in a reduced dimensional feature space compared to the dimension of the original time series signal. The researchers reported that the wavelet packet-based features, obtained by their method for vibration signals, yield 100% correct classification when used as an input to a neural network classifier.

Likewise, Sadeghian *et al.* [10] reported a novel online fault-diagnosis algorithm for induction motor mechanical fault using wavelet packet decomposition and neural networks. In their study, a new set of feature coefficients was obtained by the wavelet packet decomposition of the stator current. They used a neural network for the classification of features leading to fault detection. The proposed algorithm was also reported to be used for feature extraction in dynamical systems.

Luo *et al.* [11] condition monitoring approach on vibrational signal analysis employed wavelet filter design based on time-frequency localization of the wavelet transform. Together with autocorrelation enhancement, any number of natural frequencies in either the time or frequency domain could be observed. In this study, the peak ratio and peak value in the frequency domain were used as indicators of condition and defect.

Analyzing fault defects, many papers have addressed the removal of background noise and provided novel feature extraction techniques. The study by Chaturvedi *et al.* [12] used adaptive noise cancellation to successfully reduce the background noise. A maximum improvement of 32 dB in the signal-to-noise ratio at the output of the noise removal model was reported. Similarly, Hassanpour [13] has discussed a new approach for reducing noise from time series signals. In this study, a singular value decomposition was used to exclude the noise subspace from the signal subspace. Using Savitzky–Golay smoothing filter, the singular vectors of the matrix for the time-frequency representation were filtered. It was shown that the proposed approach had promising results in reducing noise in stationary and nonstationary signals in both time frequency and time domain. In this vein, Das *et al.* [14] proposed a computationally efficient probabilistic dependence measure for dimensionality reduction of homoscedastic and heteroscedastic data. They concluded that approximate information discriminant analysis is an alternative to the prevalent feature extraction technique.

Demitris *et al.* [15] proposed a correlation-based comparison of analog signatures for identification and fault diagnosis. They devised different criterion for automatic recognition of faulty components. Finally, Pannacchi and Vania [16] proposed a complete mathematical model of gas turbine generator unit based on correlation indexes for a small power plant to estimate the angular misalignment in flexible coupling. They computed the response of it to moments applied to the system and then compared this with a least square fit of the gas turbine generator unit at a series of frequencies. Using a combination of validated models and condition monitoring techniques, they successfully examined the behavior of the unit which had been incorrectly assembled.

Keeping with the existing research, the present paper proposes the condition monitoring of IC engine using fast Fourier transform (FFT) and correlation-based approaches. Further, to check the engine for quality, a method based on the sum of signal peaks is devised. Categorizing the particular fault [cam chain noise (CCN), cylindrical head noise (HN), magneto rotor noise (MRN), and primary gear damage (PGD)] in a faulty engine is done using correlation analysis.

## II. CBM OF IC ENGINES USING AUDIO EMISSION SIGNATURES

As mentioned earlier, the main focus in this study is on the ways of identifying a faulty engine. Sumpeak algorithm is employed to check the engine quality. It must be noted that in industrial requirements, it is permissible for any healthy engine to be declared faulty, but no faulty engine should be certified as a healthy one. Significantly, audio signatures have been used as the input for condition monitoring in many literatures [8], [9], [17]. In this regard, many diagnostic tools and methods have been developed with much success. Sensor fusion techniques are also commonly employed due to the inherent benefits in taking advantage of mutual information from multiple sensors [18]. Notably, the decision making in CBM focuses on predictive maintenance. Moreover, the basic formulation of condition monitoring has been the same as **data**

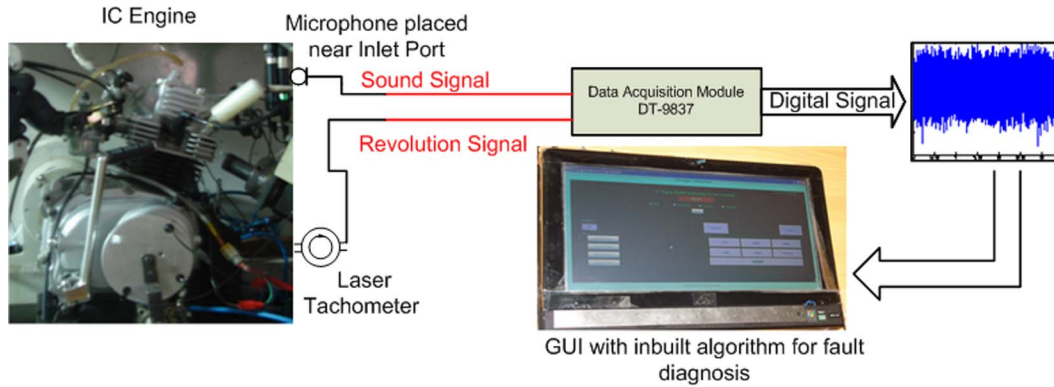


Fig. 2. Experimental Setup.

### acquisition, data preprocessing, data analysis, and data classification.

#### A. Malfunctioning in IC Engines

Amongst the defective engines, the acquisition of audio signature of engines was required with the following principal defects:

- 1) cam chain noise (CCN);
- 2) cylinder head noise (CHN);
- 3) magneto rotor noise (MRN);
- 4) primary gear damage (PGD).

In the succeeding paragraphs, an investigation of each of these faults is presented.

**Cam chain noise:** The cam chain is the element within the engine that transfers the drive from the crank shaft to the cam shaft. The tension on the cam chain can be adjusted by pushing the slider inward or outward. This can be done using the tension adjuster which is accessible. Whenever the cam chain is either excessively tight or loose, it produces the cam chain noise. All cam chain noise faults are seeded by varying the tension on the cam chain using the tension adjuster.

**Cylinder head noise:** Inappropriate setting of the top dead center results in slapping of the cylinder head which gives rise to cylinder head noise. The cylinder head fault was seeded by deforming/machining the surface of the cam shaft.

**Primary gear damage:** The gear assembly is located within the crank case and comprises a set of drive gear and driven-gear assemblies. Any abnormality in these gear assemblies in the form of tooth damage, tooth to tooth error, or eccentric/inclined bore, results in typical impact kind of noises. The primary gear damage problem was seeded by individually introducing defects (tooth damage) in the drive gear and the driven gear.

**Magneto rotor noise:** The stator, in conjunction with the rotor (big brass-like looking thing, located under the left engine cover) that covers it, is responsible for the spark, lighting, and charging system. Under the rotor, there are three coils: the source, the pulsar, and the lighting/charge coils. The source coil allows a spark to be generated, the pulsar tells the engine when to make a spark at the spark plug, the

lighting generates the voltage to light the headlight, and the charge coil charges the battery. The gaps around the pulsar coil are fixed. If by any means this gap is decreased, the coil starts rubbing and produces a noise; this noise is known as the magneto rotor noise. This can also be generated if the pulsar coil's screws are loose which, of course, is a very rare condition.

### III. PROPOSED METHOD AND EXPERIMENTAL SETUP

Based on a statistical approach, the methodology can be described as a hypothesis test problem with

$$H_0 = \text{Fault is present}$$

$$H_1 = \text{Engine is healthy.}$$

$H_0$  and  $H_1$  can be interpreted into statistical expression using specific rules, models, or distributions. Test statistics is then computed to summarize the condition of engine so as to decide whether the hypothesis  $H_0$  is true or not. Hypothesis testing for fault diagnosis has also been discussed in [19], [20].

The distinction between a healthy engine and faulty engine is made by a Sumpeak algorithm discussed later in the section. Therefore, it can be emphasized that the hypothesis  $H_0$  is always true while identifying the fault/s in faulty engines.

For identifying fault/s in faulty engines, our motivation for using correlation as a certificatory tool comes from the fact that any unknown engine audio sample can be matched with a set of ideal faulty engines. In this regard, it has also been observed that working in the time domain poses many problems such as insufficient information and noise embedding in certain frequency pockets. This is resolved by taking the Fourier transform of the signal to analyze it in the frequency domain. As mentioned in the literature [9], wavelet-based or time-frequency-based approaches can be used for classification. However, it can be claimed that frequency-based approaches have not been fully exhausted and utilized. Accordingly, this paper demonstrates that statistical-based feature extraction techniques can also be very well used in industrial situations for classification and optimum working of CBM.

Fig. 2 shows the actual experimental setup used to collect, synthesize, and analyze data. Here, the touch screen panel has a user-friendly interface. The data acquisition board DT-9837

TABLE I  
ENGINE SAMPLES RECORDED FOR VARIOUS FAULTS

S. No.	Fault	Total Engines
1	Healthy Engine	110
1	Cam Chain Noise (CCN)	110
2	Cylinder Head Noise (CHN)	100
3	Magneto Rotor Noise (MRN)	120
4	Primary Gear Damage (PGD)	160

is used to collect engine audio signals. Since the arrival rate of faulty engines was observed to be very low, it became necessary to seed the faults in the engine. Following this approach, 600 engine samples were collected of which 490 are defective engine samples. The individual break up of healthy and fault-seeded engines is tabulated in Table I.

Following a practical approach in describing the present experimental setup, this paper first discusses the general framework for the entire process and simultaneously relates it with the actual parameters used in the analysis.

#### A. System Specification

In this paper, PCB 130D20 piezoelectric microphones were used for the collection of audio signatures. Owing to their robustness and high temperature variability, these microphones are generally preferred over others for industrial purposes. Likewise, for data acquisition purposes, a data translation (DT-9837) board was used. Notably, this board has a tachometer input which triggers the whole data acquisition circuitry only at a particular speed (in revolution per minute). Also, LabVIEW 8.2 version was used for data acquisition. Subsequently, the data acquired through this process is in the “.dat” format and is ready for analysis. Since the maximum frequency for the engine state can be 12 kHz, the Nyquist criterion sampling frequency was employed at 50 kHz. Observably, a typical audio sample has a bit rate of 128 kb/s with monochannel. For the present analysis, the data used is taken within a particular speed band which is 2800–3200 rpm.

#### B. Audio Analysis of IC Engine: Specifications and Difficulties

Many literatures [8], [9] analyze their methodology on data that is either created artificially or being used as a standard data set instead of the ones obtained under theoretical circumstances satisfying some of the basic properties of noise embedding in signals. In the present study, the data are recorded under actual industrial conditions where the sound from other engines as well as human sounds also contribute to the signal while recording the incoming engine's sound. Moreover, regular large sound impulse is also common in automobile industries. Accordingly, preprocessing of such signals is indeed a challenge. Therefore, a general framework for all the recording of engines has been followed in this study. Faulty engines were either artificially seeded, or any incoming faulty engine that came during the engine assembly was taken for recording. Hereafter, all the

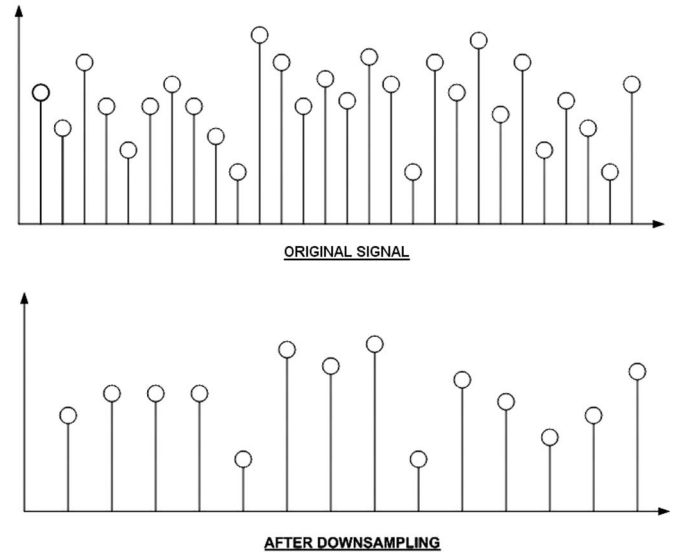


Fig. 3. Illustration of the Downsampling Process With  $M = 2$ .

recordings were done for a 10-s time frame. This large band was necessary to measure the regular sound burst. It was also observed that if the sound burst appeared in one time frame and suppressed the required feature, then by using a large frame (10 s), the feature to be extracted would again reappear in the next frame.

#### C. Preprocessing of Audio Signals

In the present study, the data preprocessing is mainly concerned with the filtering and downsampling of the acquired data. Next, band pass filter with pass band frequencies of the range 800–12 500 Hz is used. The incoming signal received is, thus, mean-variance normalized and passes through the band pass. Further, downsampling is carried out which is the process of reducing the sampling rate of the signal. This is usually done by reducing the data rate or its size. Precisely, downsampling is done by keeping every  $M_0^{th}$  sample of  $x[n]$  and removing  $M_0-1$  in-between samples, thereby generating an output sequence  $y[n]$  according to the relation

$$y[n] = x[nM_0] \quad (1)$$

where  $M_0$  is an integer factor and  $M_0 > 1$ . This results in a sequence  $y[n]$  whose sampling rate is  $(1/M_0)$ th that of  $x[n]$ . Fig. 3 shows the diagrammatic illustration of the above procedure.

#### D. Sumpeak Algorithm for Classifying Healthy/Faulty Engines

To identify the incoming engine as healthy or faulty, a Sumpeak algorithm is designed which essentially uses the Hilbert transform (HT) at its core. HT is a time-domain convolution that maps one real-valued time history onto another. It is defined as [21]

$$H[x(t)] = \frac{1}{\pi} \int_{-\infty}^{\infty} \frac{y(t)}{t - \tau} \quad (2)$$



TABLE II  
FREQUENCY BAND FOR DIFFERENT FAULTS

S. No.	Fault	Frequency Band
1	CHN	3.5-4.5 kHz
2	PGD	2-3 kHz
3	CCN& MRN	0.5-2 kHz

where  $t$  is the time,  $y(t)$  is a time-domain signal, and  $H[y(t)]$  is the Hilbert transform of  $y(t)$ . Since Hilbert transform is a frequency-independent  $90^\circ$  phase shifter, the nonstationary characteristics of the modulating signal are not affected by this method. Moreover, amplitude and phase modulation function,  $p_m(t)$  and  $q_m(t)$ , respectively, can be extracted by Hilbert transform [22]. Demodulation is accomplished by forming a complex-valued time-domain signal called the analytic signal,  $Q[y(t)]$ , which is defined as

$$Q[y(t)] = y(t) + iH[y(t)] = q(t)e^{j\phi(t)}, \quad i = \sqrt{-1}. \quad (3)$$

The resulting complex time-domain signal can be converted from the real/imaginary format to the magnitude/phase format as presented below

$$e(t) = \sqrt{y^2(t) + H^2[y(t)]} \quad (4)$$

$$\phi(t) = \arctan \frac{H[y(t)]}{y(t)}. \quad (5)$$

Hilbert transform produces a complex time series. The envelope is the magnitude of this complex time series and represents an estimate of the modulation present in the signal due to sidebands [23].

To illustrate the procedure for the Sumpeak algorithm, the input audio sample is clipped for 1 s, downsampled and normalized to 25 kHz with 25 000 sample points. The clipped audio sample is divided into three bands using band pass filters with pass band frequencies (0.5–2 kHz, 2–3 kHz, and 3.5–4.5 kHz) as mentioned in [24]. Basically, in the preliminary analysis, it is seen that the studied faults appear in the range between 0.5 and 4.5 kHz. The individual frequency bands in which the four studied faults appear are tabulated in Table II. The purpose of band pass filtering is to reject the low-frequency high-amplitude signals associated with imbalance and misalignment and to eliminate the random noise outside the pass band [25]–[27]. After the band pass filtering and envelope analysis using Hilbert transform are done, local maxima or peaks of the envelope are computed. Each value of the envelope  $e(t)$  is hereafter compared with its neighboring value [28], and if it is larger than both of its neighbors, it is considered a peak.

The envelope  $e(t)$  of the three-band passed-filtered signals are extracted using the Hilbert transform. Peaks of the envelopes are calculated as follows.

- 1) Find the first derivative  $d_1$  of the envelope  $e(t)$

$$d_1 = \begin{cases} 1, & \text{if } \frac{\partial e}{\partial t} > 0 \\ 0, & \text{Otherwise} \end{cases}. \quad (6)$$

- 2) Find the second derivative  $d_2$  of the envelope

$$d_2 = \begin{cases} 1, & \text{if } \frac{\partial d_1}{\partial t} > 0 \\ 0, & \text{Otherwise} \end{cases}. \quad (7)$$

The positions at which the second derivative is one are marked as peaks. Sum of the peaks (SOP) is calculated as follows:

$$SOP = \sum_{d_2} e_{d_2}. \quad (8)$$

Fig. 4 shows the schematic diagram of the Sumpeak algorithm for detecting the healthy engines.

#### E. Preparing Audio Samples for Correlation Analysis: Algorithm for Faulty Engine Detection

Correlation function of the baseline (prototype) and real time (unknown) signals is used to investigate the relationship between them. There are applications where it is necessary to compare one reference signal with other signals to determine both the similarity between the pair and the additional information based on the similarity. A measure of similarity between a pair of signal,  $x[n]$  and  $y[n]$ , is given by the *cross-correlation sequence*  $r_{xy}[l]$  defined by

$$r_{xy}[l] = \sum_{n=-\infty}^{\infty} x[n]y[n-l], \quad l = 0, \pm 1, \pm 2, \dots \quad (9)$$

The parameter “ $l$ ,” called *lag*, indicates the time shift between the pair. The time sequence  $y[n]$  shifts by  $l$  samples with respect to the reference sequence  $x[n]$  to the right for positive values of  $l$  and shifts  $l$  samples to the left for the negative values of  $l$ .

The *autocorrelation* sequence of  $x[n]$  is given by

$$r_{xx}[l] = \sum_{n=-\infty}^{\infty} x[n]x[n-l] \quad (10)$$

obtained by setting  $y[n] = x[n]$  in (9).

Here, the expression for cross correlation looks quite similar to that of the convolution. The cross correlation of the sequence  $x[n]$  with the reference sequence  $y[n]$  can be computed by processing  $x[n]$  with a linear time invariant (LTI) discrete-time system of impulse response  $y[-n]$ . Likewise, the autocorrelation of  $x[n]$  can be determined by passing it through an LTI discrete-time system of impulse response  $x[-n]$ .

The normalized form of *autocorrelation* and *cross correlation* is given by

$$\rho_{xx}[l] = \frac{r_{xx}[l]}{r_{xx}[0]} \quad (11)$$

$$\rho_{xy}[l] = \frac{r_{xy}[l]}{\sqrt{r_{xx}[0]r_{yy}[0]}}. \quad (12)$$

The possible range of  $\rho_{xy}[l]$  is  $|\rho_{xx}[l]| \leq 1$  and  $|\rho_{xy}[l]| \leq 1$ , independent of the range of values of  $x[n]$  and  $y[n]$ , and a value of one indicates the highest correlation coefficient as a result of the corollary of the Cauchy–Schwarz inequality.

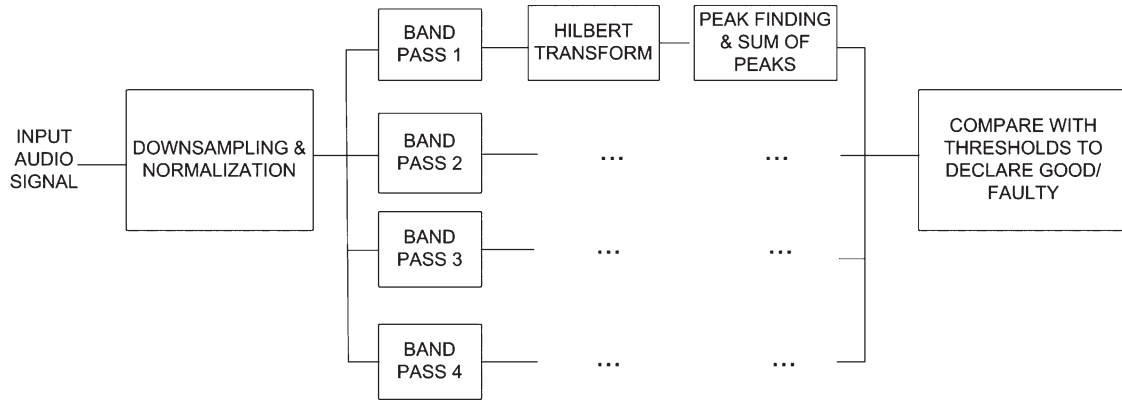


Fig. 4. Flow Diagram for Sumpeak Algorithm.

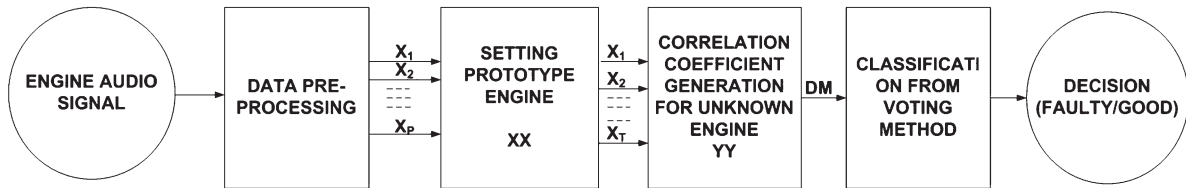


Fig. 5. Flow Diagram for correlation-based faulty engine classification.

In probability theory and in statistics, the term *correlation coefficient* shows the linear relationship between two random variables. In general statistical parlance, correlation refers to the departure of two random variables from independence. There are several coefficients, measuring the degree of correlation, adapted to the nature of the data.

A number of different coefficients are used for different situations. The best known is the Pearson product-moment correlation coefficient, which is obtained by dividing the covariance of the two variables by the product of their standard deviations.

The correlation coefficient  $\rho_{X,Y}$  between two random variables  $X$  and  $Y$  with expected values  $\mu_X$  and  $\mu_Y$  and standard deviations  $\sigma_X$  and  $\sigma_Y$  is defined as

$$\rho_{X,Y} = \frac{E((X - \mu_X)(Y - \mu_Y))}{\sigma_X \sigma_Y} \quad (13)$$

where  $E$  is the expected value operator.

**Calculating a Set of Prototype Engine:** Fig. 5 shows the flow diagram used for correlation coefficient-based faulty engine classification. The first step in the preparation of samples involves the breaking of preprocessed signal into “ $q$ ” number of windows each of “ $w$ ” samples. The value of “ $w$ ” is selected such that it captures “ $r$ ” mechanical revolution of engine. The second step is to map each window in frequency domain using Fourier transform. At the end of second step “ $q$ ,” such frequency spectrum is available. Each spectrum is again divided into “ $k$ ” number of bins, and each bin contains average value of corresponding FFT points.

The aforementioned step is necessary before a correlation analysis. Time-domain information is not able to sufficiently capture the useful information in terms of its interdependence within and outside its class.

In this case, the engine speed has been taken at 3000 rpm at a sampling frequency of 50 kHz with 10-s audio signal containing

500 000 samples of data. After downsampling by two, the data points become 250 000. From this information, it is concluded that the engine makes approximately four revolutions and contains 2000 samples. This signal for four revolutions of the engine is taken from the whole signal. Since the faults being considered here are periodic in nature, it helps in the aforementioned process. Moreover, in taking a 2000-sample window frame, a periodic signal is considered for analysis.

In this process, the audio signal is linearly normalized, and owing to its large data size, it is downsampled. Further, ten windows with 50% overlap is used such that each window captures four revolutions of the engine. Now, for each window, Fourier transform is computed using predefined Matlab function *fft*. To obtain the sharpness of the frequency content in the signal, FFT with a length of 75 000 points is computed. The number of FFT points is in the next power of two. The logic behind taking this length of the FFT is that the discrete Fourier transform is an approximate case of continuous Fourier transform. Taking a large set of data points eventually helps in the approximation of the signal toward a continuous case. Following extensive experimental work, the time-domain signal is downsampled and divided into windows of 2000 data points each, with a total of ten windows. Now, the Fourier transform for each window is calculated, and for each window, 120 frequency bins are obtained. Each bin contains 100 Fourier transform points, and after taking the mean values of these 100 points, the final 120 points are considered for further analysis.

Having calculated the spectrum, prototype or standard model engine is computed first to form a set of engines which further helps in the analysis of any unknown engine to determine its condition. For all the engines, a correlation coefficient matrix  $X_{cor}$  is computed comprises of correlation values between inter- and intragroup of faulty engines. Hereafter, this  $X_{cor}$  is divided into inter- and intrafault matrices where each intrafault matrix has autocorrelation values, and each interfault matrix

shows cross correlation values. A set of engines is then tabulated which crosses certain correlation coefficient threshold value. The engines whose correlation coefficient values cross maximum times, the threshold values are considered as prototype engines.

Considering  $X_{cor}$  as the correlation coefficient matrix as mentioned above, two types of correlation coefficients are calculated, intra and inter. For the present analysis, it is required to deal the problem with a dual perspective. This includes a strong correlation coefficient within a category of fault (intra) and a least correlation between different faults (inter). Also, optimization is an important process in any system built for real-time applications. Hence, necessary measures are taken to decrease the processing time. To ease the computation, the commutative property of correlation is used, and computational time is saved by calculating the correlation only for the upper diagonal of the correlation coefficient matrix. Since the principal elements are also the correlation for the same engine sample, these elements do not require further calculation. Accordingly, the process can be speeded up at an incremental rate. Now, based on correlation coefficient values, engines whose values exceed threshold values  $\lambda_1$  and  $\lambda_2$  for both intra- and interfaults, respectively, are computed. Generally, engines which satisfy the criterion for  $\lambda_1$  also at the same time satisfy the  $\lambda_2$  criterion. The values obtained from experimental analysis in the present study are  $\lambda_1 = 0.8$  and  $\lambda_2 = 0.65$ . These values are empirically chosen based on the accuracy of the results for this research. However, they would be different for different applications. Thus, considering the above criterion, a set of prototype engines is computed which serves as comparison models for unknown set of engines. The quality of classification system highly depends upon this set of prototype engines and is to be carefully chosen.

Fig. 6 illustrates the overall methodology. (A) is the time-domain mean-variance normalized signal. (B) is the sliced signal corresponding to four revolutions. (C) is the FFT of the signal in (B). Slicing (C) in the frequency bins and taking median values will result in (D).

#### F. Unknown Faulty Engine Classification

Any unknown engine will first go through a Sumpeak algorithm which checks whether the engine is healthy or faulty. If it appears faulty, further processing using correlation analysis is carried out.

A set of prototype engines whose correlation coefficient matrix  $X$  is formed in the preceding section is now put into use. The unknown engine frequency spectrum is calculated as explained in the previous section. Subsequently, correlation coefficient matrix is calculated to check the proximity with each fault of engine sample.

For the rest of the section, it is assumed that the unknown engine has passed through the Sumpeak algorithm and is faulty. The rest of the analysis is done keeping this assumption in mind. The unknown engine time-domain signal is processed along the same line as described in the preprocessing of audio signal in the previous subsection. The correlation coefficient values are then calculated between the unknown engine sample

and all other prototype engines. Finally, a decision matrix  $DM$  whose rows are the different types of faults and columns as the number of windows is left for the analysis of the particular fault present in the engine.

$$DM = \begin{bmatrix} x_{1,1} & x_{1,2} & \cdots & x_{1,10} \\ \vdots & \ddots & \ddots & \vdots \\ \vdots & \cdots & \ddots & \vdots \\ x_{4,1} & \cdots & \ddots & x_{4,10} \end{bmatrix}. \quad (14)$$

#### G. Voting System

The matrix  $DM$  obtained above has correlation values for ten windows in its columns and the corresponding values for each type of classification (four in this case) in its rows.

The average values across the rows are now calculated, thus producing the mean value of the windows corresponding to all the faults. This matrix is called as *windavg*

$$windavg = \begin{bmatrix} m_{1,1-10} \\ \vdots \\ m_{i,1-10} \\ \vdots \\ m_{4,1-10} \end{bmatrix} \quad (15)$$

where each element in *windavg* represents the mean value calculated across the rows.

It would be a waste of resources if only the maximum value of  $DM$  is reported as the fault, and the rest is discarded as in the case normally. Further, it is advantageous to fuse the decision of other faults if they fall within a permissible numerical limit. This strategy is analogous to combining the decision of two skilled operators to form a reliable and robust classification system. Moreover, this is also supported by several other literatures [4], [5] which combine other statistical and intelligence techniques to show diverse generalization.

After this, first and second maximum values are calculated in this matrix and a term  $\alpha$  which is defined as the difference between the first two maximum terms of the matrix. If this  $\alpha$  is less than a threshold value, which is 0.25 in this case, then it can be declared that the unknown engine sample has two faults, else the engine is said to have only one fault. The theory applied here needs some explanation from a practical viewpoint. During the data collection process, it has been observed that some of engines can have more than one fault. It is also noted that even skilled technicians reporting the condition of the engines differ from one another. Although, both faults may be present in the system, depending upon the interpretation of a technician, the fault reported minor by one can be called major by the other and vice versa.

## IV. RESULTS

In the present study, the feasibility of the algorithm is examined on the real data set collected from a leading automobile company in India. Of the 600 engine samples used here, 110 were healthy of which 100 engine samples were giving

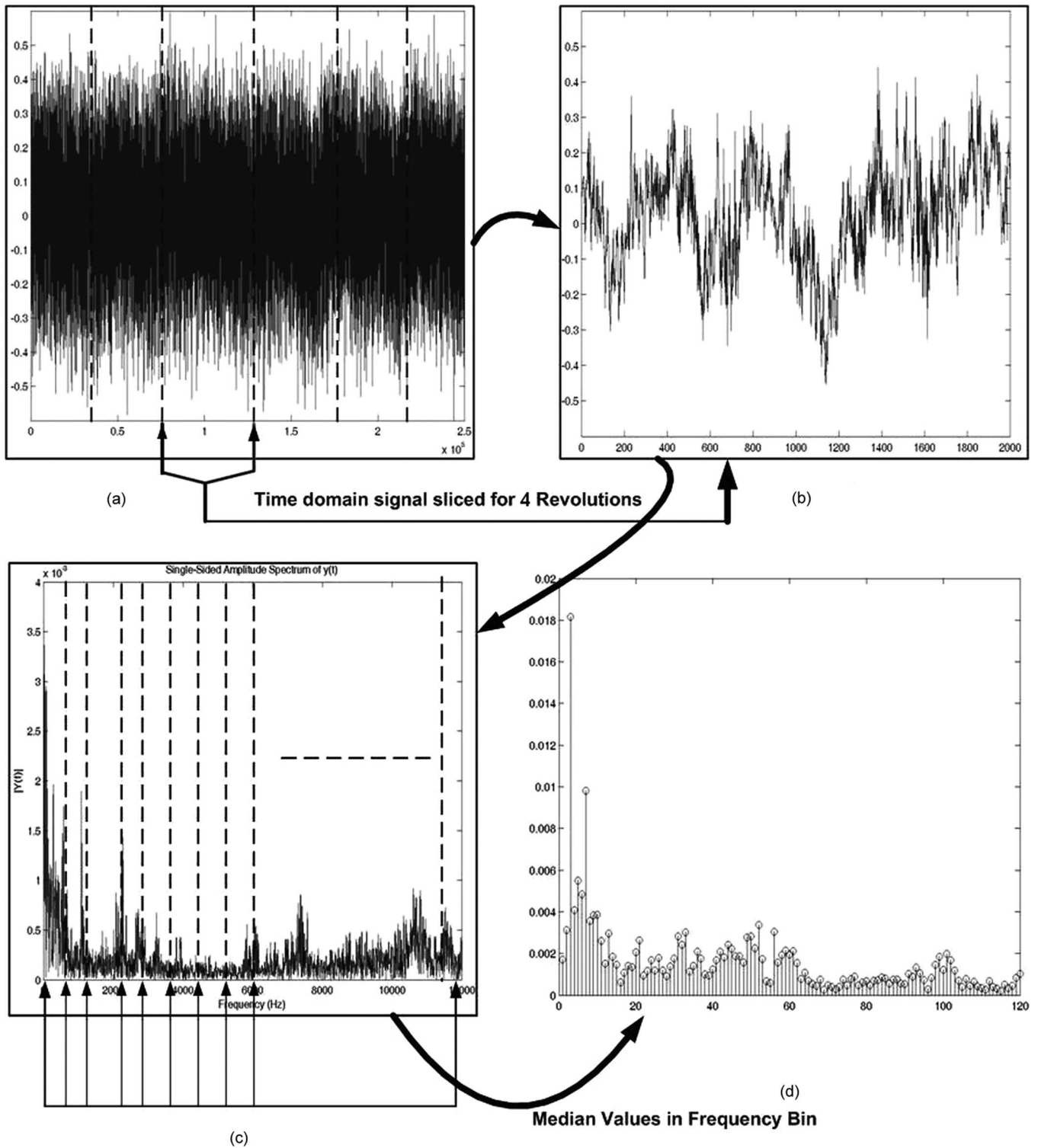


Fig. 6. Correlation-Based Faulty Engine Classification.

91% correct classification from Sumpeak algorithm. The prototype engines are chosen from the remaining 490 engines, and then, the results are processed based on the outcome of the classification scheme. If any one of the two faults is properly diagnosed, then it is reported as the correct classification. The classification accuracy for the studied faults are given below.

- 1) 110 engines having CCN fault were tested, and 91 were declared as CCN fault by giving 82% accuracy.

- 2) 100 engines having CHN fault were tested, and 80 of them were declared as CHN fault by giving 80% accuracy.
- 3) 120 engines of MRN fault were tested, and 109 of them were declared as MRN fault, so the accuracy of MRN fault detection is 93%.
- 4) 160 engines of PGD fault were tested, and 134 of them were declared as PGD fault, so the accuracy of PGD fault detection is 83%.



## V. CONCLUSION

The proposed method on Sumpeak analysis for classification between healthy and faulty classes and the correlation-based analysis for classifying faulty engines in its respective fault class clearly indicate the effectiveness for detecting the faults in IC engines. The prototype-based matching of the audio signature of the engine of unknown class with the known class prototype engines has shown a significant improvement in the online condition monitoring and fault diagnosis of IC engine in actual industrial environment. Most literature dealing with fault diagnosis of IC engine has applied their methods under laboratory environments and proposed that their algorithms can be used for online fault diagnosis under actual industrial environment. In the present research, the proposed technique carried out online fault diagnosis of IC engine under actual industrial environment with desirable accuracy and specified time limits. The proposed scheme has been tested in online fault diagnosis of IC engine in one of the prominent two-wheeler manufacturing companies in India. Online testing was conducted with 1.6-GHz processor and 2-GB memory. Analysis time of one engine is varied from 1.5 to 2 s with desirable accuracy and repeatability. Conventionally, this testing was done by an expert technician in 60 to 120 s. Also, the proposed method works satisfactorily for engines having a maximum of two faults at the same time.

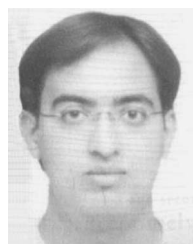
## REFERENCES

- [1] H. P. Bloch and F. K. Geitner, *Machinery failure Analysis and Trouble Shooting*. Houston, TX: Gulf, 1997.
- [2] J. Liu, W. Wang, and F. Golnaraghi, "An extended wavelet spectrum for bearing fault diagnostics," *IEEE Trans. Instrum. Meas.*, vol. 57, no. 12, pp. 2801–2812, Dec. 2008.
- [3] R. Yan and R. Gao, "Rotatory machine health diagnosis based on empirical mode decomposition," *Trans. ASME, J. Vib. Acoust.*, vol. 130, pp. 1–12, 2008.
- [4] A. J. C. Sharkey, "Combining artificial neural nets," *Connection Sci.*, vol. 8, no. 3/4, pp. 299–314, Dec. 1996.
- [5] A. J. C. Sharkey, Ed., *Combining Artificial Neural Nets: Ensemble and Modular Multi-Net Systems*, 1st ed. London, U.K.: Springer-Verlag, 1999.
- [6] X. Fan and M. J. Zuo, "Gearbox fault detection using Hilbert and Wavelet packet transform," *Mech. Syst. Signal Process.*, vol. 20, no. 4, pp. 966–982, May 2006.
- [7] Q. Sun, P. Chen, D. Zhang, and F. Xi, "Pattern recognition for automatic machinery fault diagnosis," *Trans. ASME, J. Vib. Acoust.*, vol. 126, pp. 307–316, 2004.
- [8] C. Bunks, D. McCarthy, and T. Al-Ani, "Condition-based maintenance of machines using hidden Markov models," *Mech. Syst. Signal Process.*, vol. 14, no. 4, pp. 597–612, Jul. 2000.
- [9] G. G. Yen and K. C. Lin, "Wavelet packet feature extraction for vibration monitoring," *IEEE Trans. Ind. Electron.*, vol. 47, no. 3, pp. 650–666, Jun. 2000.
- [10] A. Sadeghian, Z. Ye, and B. Wu, "Online detection of broken rotor bars in induction motors by wavelet packet decomposition and artificial neural networks," *IEEE Trans. Instrum. Meas.*, vol. 58, no. 7, pp. 2253–2263, Jul. 2009.
- [11] G. Y. Luo, D. Osypiw, and M. Irle, "Real time condition monitoring by significant and natural analysis of vibration signal with wavelet filter and autocorrelation enhancement," *J. Sound Vib.*, vol. 236, no. 3, pp. 413–430, Sep. 2000.
- [12] G. K. Chaturved and D. W. Thomas, "Adaptive noise canceling and condition monitoring," *J. Sound Vib.*, vol. 76, no. 3, pp. 391–405, Jun. 1981.
- [13] H. Hassanpour, "A time-frequency approach for noise reduction," *Dig. Signal Process.*, vol. 18, no. 5, pp. 728–738, Sep. 2008.
- [14] K. Das and Z. Nenadic, "Approximate information discriminant analysis: A computationally simple heteroscedastic feature extraction technique," *Pattern Recognit.*, vol. 41, no. 5, pp. 1548–1557, May 2008.
- [15] D. K. Papakostas and A. A. Hatzopoulos, "Correlation-based comparison of signatures for identification and fault diagnosis," *IEEE Trans. Instrum. Meas.*, vol. 42, no. 4, pp. 860–863, Aug. 1993.
- [16] A. Vania and P. Pennacchi, "Experimental and theoretical application of fault identification measures of accuracy in rotating machine diagnostics," *Mech. Syst. Signal Process.*, vol. 18, no. 2, pp. 329–352, Mar. 2004.
- [17] M.-C. Pan, P. Sas, and H. Van Brussel, "Machine condition monitoring using signal classification techniques," *J. Vib. Control*, vol. 9, no. 10, pp. 1103–1120, Oct. 2003.
- [18] R. J. Hansen, D. L. Hall, and S. K. Kurtz, "A new approach to the challenge of machinery prognostics," *J. Eng. Gas Turbines Power*, vol. 117, no. 2, pp. 320–325, 1995.
- [19] J. Ma and C. J. Li, "Detection of localized defects in rolling element bearings via composite hypothesis test," *Mech. Syst. Signal Process.*, vol. 9, no. 1, pp. 63–75, Jan. 1995.
- [20] H. Sohn, K. Worden, and C. R. Farrar, "Statistical damage classification under changing environmental and operational conditions," *J. Intell. Mater. Syst. Struct.*, vol. 13, no. 9, pp. 561–574, Sep. 2002.
- [21] A. Carcaterra and A. Sestieri, "Complex envelope analysis: A quasi static approach to vibrations," *J. Sound Vib.*, vol. 201, no. 2, pp. 205–233, Mar. 1997.
- [22] P. D. McFadden, "Detecting fatigue cracks in gears by amplitude and phase demodulation of the meshing vibration," *Trans. ASME, J. Vib. Acoust. Stress Reliab. Des.*, vol. 108, pp. 165–170, 1986.
- [23] J. J. Zakrajsek, R. F. Handschuh, D. G. Lewicki, and H. J. Decker, "Detecting gear tooth fracture in a high contact ratio face gear mesh," in *Proc. 49th Meeting Mech. Failure Prevention Group*, Virginia Beach, VA, Apr. 18–20, 1995.
- [24] L. Sriram, "Audio based condition monitoring and fault diagnosis of Internal Combustion Engine," M.S. thesis, Dept. Elect. Eng., Indian Inst. Technol., Kanpur, India, 2008.
- [25] R. M. Jones, "Enveloping for bearing analysis," *J. Sound Vib.*, vol. 30, pp. 10–15, 1996.
- [26] *Revolutions, Special Edition on Bearing Monitoring*, vol. 7, San Diego, CA.
- [27] S. A. McInerny and Y. Dai, "Basic vibration signal processing for bearing fault detection," *IEEE Trans. Educ.*, vol. 46, no. 1, pp. 149–156, Feb. 2003.
- [28] N. V. Novik, "Analysis of the feasibility of diagnosing an internal combustion engine based on chronometric measurements," *Meas. Tech.*, vol. 42, no. 1, pp. 49–52, Jan. 1999.



**Sandeep Kumar Yadav** received the B.Tech. degree from Harcourt Butler Technological Institute Kanpur, Kanpur, India and the M.Tech. degree from the Indian Institute of Technology Kanpur, Kanpur, India, where he is currently working toward the Ph.D. degree in the Department of Electrical Engineering.

His area of research includes signal processing, image processing, and condition monitoring.



**Kanishka Tyagi** received the B.Tech. degree in electrical engineering from the G.B. Pant University of Agriculture and Technology, Pantnagar, India, in 2008. He is currently a M.S. student in the Image Processing and Neural Networks Lab, University of Texas at Arlington, Arlington.

From 2008 to 2009, he was a Research Associate with the Department of Electrical Engineering, Indian Institute of Technology Kanpur, Kanpur, India. His current research interests are nonlinear neural networks, wavelet theory, and signal

processing.



**Brijeshkumar Shah** received the M.Tech. degree in electrical engineering from the Indian Institute of Technology (IIT) Kanpur, Kanpur, India, in 2009.

He is currently working with the Department of Electrical Engineering, IIT, as a Senior Research Associate. His research interests are image and acoustic signal processing, fuzzy logic-based systems, and data acquisition process.



**Prem Kumar Kalra** (SM'91) was born in Agra, India, on October 25, 1956. He received the B.Sc. (Engg.) degree from Dayalbagh Educational Institute, Agra, India, in 1978, the M.Tech. degree from the Indian Institute of Technology (IIT) Kanpur, Kanpur, India, in 1982, and the Ph.D. degree from Manitoba University, Winnipeg, MB, Canada, in 1987.

He was an Assistant Professor with the Department of Electrical Engineering, Montana State University, Bozeman, from January 1987 to June 1988.

In July–August 1988, he was a visiting Assistant Professor with the Department of Electrical Engineering, University of Washington, Seattle. Since September 1988, he has been with the Department of Electrical Engineering, IIT Kanpur. He was a Professor and Head of the Department of Electrical Engineering, IIT Kanpur. He is currently the Director of the IIT, Rajasthan, India. He has published over 150 papers in reputed national and international journals and conferences. His research interests are fuzzy logic, neural networks, image processing, computational neuroscience, condition monitoring, and intelligent systems.

Dr. Kalra is a Fellow of the Institution of Electronics and Telecommunication Engineers and a Life Member of the Institution of Engineers, India.